Translation Eukaryotic Initiation Factor 4G Recognizes a Specific Structural Element within the Internal Ribosome Entry Site of Encephalomyocarditis Virus RNA*

Victoria G. Kolupaeva‡§, Tatyana V. Pestova‡§, Christopher U. T. Hellen§, and Ivan N. Shatsky‡¶

From the ‡A. N. Belozersky Institute of Physico-Chemical Biology, Moscow State University, 119899 Moscow, Russia and §Department of Microbiology and Immunology, Morse Institute for Molecular Genetics, State University of New York Health Science Center at Brooklyn, Brooklyn, New York 11203-2098

A complex of eukaryotic initiation factors (eIFs) 4A, 4E, and 4G (collectively termed eIF4F) plays a key role in recruiting mRNAs to ribosomes during translation initiation. The site of ribosomal entry onto most mRNAs is determined by interaction of the 5′-terminal cap with eIF4E; eIFs 4A and 4G may facilitate ribosomal entry by modifying mRNA structure near the cap and by interacting with ribosome-associated factors. eIF4G recruits uncapped encephalomyocarditis virus (EMCV) mRNA to ribosomes without the involvement of eIF4E by binding directly to the ~450-nucleotide long EMCV internal ribosome entry site (IRES). We have used chemical and enzymatic probing to map the eIF4G binding site to a structural element within the J-K domain of the EMCV IRES that consists of an oligo(A) loop at the junction of three helices. The oligo(A) loop itself is not sufficient to form stable complexes with eIF4G since alteration of its structural context abolished its interaction with eIF4G. Addition of wild type or *trans*-dominant mutant forms of eIF4A to binary IRES·eIF4G complexes did not further alter the pattern of chemical/enzymatic modification of the IRES.

Initiation of protein synthesis in eukaryotes involves the sequential binding of small (40 S) and large (60 S) ribosomal subunits to an mRNA, leading to the assembly of an 80 S initiation complex at the initiation codon (1). The rate-limiting step in this process is recruitment of mRNAs to the 43 S preinitiation complex, which consists of the 40 S ribosomal subunit, methionine-initiator tRNA, and initiation factors, including eIF2[1] and eIF3. Ribosomal recruitment to most mRNAs requires the m⁷GpppN cap structure at the 5′ end of the mRNA (2), but ribosomal binding to a smaller number of mRNAs is cap- and end-independent, and is instead mediated by an IRES in the 5′-untranslated region (3). One group of IRES elements is exemplified by encephalomyocarditis virus (EMCV) RNA (4). EMCV is a member of the cardiovirus genus of the Picornaviridae family.

Eukaryotic initiation factor eIF4F, which consists of eIF4A, eIF4E, and eIF4G subunits, plays the central role in recruiting mRNAs to 43 S complexes during initiation. The cap structure is recognized by the 24-kDa cap-binding protein eIF4E. eIF4A is an RNA-dependent ATPase/RNA helicase that is thought to unwind cap-proximal regions of the 5′- untranslated region of an mRNA, permitting attachment of the 43 S complex (1, 2). The 154-kDa eIF4G subunit of eIF4F binds to these and other factors, thereby coordinating and enhancing their activities. eIF4E associates with amino acid residues 411–428 of eIF4G, eIF3 binds to the central part of eIF4G (residues 486–886), and eIF4A binds to sites in the central and in the C-terminal thirds of eIF4G (5–7). eIF4G enhances binding both of eIF4E to the cap and of eIF4A to RNA (8, 9). The modular nature of eIF4G supports a model in which it acts as a bridge between the mRNA cap (via eIF4E) and the 40 S subunit (via eIF3, a constituent of the 43 S preinitiation complex) (6). In addition to containing binding sites for these factors, eIF4G contains sequences in its center (7, 10, 11) that are characteristic of RNA binding domains (RBDs) (for review, see Burd and Dreyfuss (12)). A role for this putative RBD in cap-mediated initiation of translation has not been elucidated, but it could contribute to the cap-binding, RNA-binding, and RNA helicase activities of eIF4F (8, 9, 13).

Recently, substantial evidence has implicated eIF4F in cap-independent, IRES-mediated translation initiation of some viral mRNAs (9, 14–17). One function of eIF4F in this process is to enable eIF4A to enter the mRNA-43 S ribosomal preinitiation complex (16). A second function, first identified using EMCV mRNA, is to directly recognize and bind to the IRES (9, 17). This interaction requires the central third of eIF4G, including the putative RBD, and is independent of eIF4A and eIF4E (17). The requirement for eIF4F in EMCV translation can be met by eIF4A and this central RBD-containing domain of eIF4G (9). We have suggested that this specific RNA binding activity of eIF4G may substitute for the cap-binding role of eIF4E in recruiting mRNAs to 40 S subunits (9, 17). In this model, the IRES has an analogous function in the translation process to the 5′-terminal cap; these RNA structures both bind to eIF4F, thereby recruiting 40 S subunits to a specific site on an mRNA. This RNA binding activity of eIF4G could therefore regulate gene expression by facilitating selective translation of cellular IRES-containing mRNAs under conditions when eIF4E is inactive.

Cellular and viral IRESs are large, complex RNAs, and can be assigned to different groups on the basis of sequence and structural similarities. Conserved structural elements may correspond to binding sites for initiation factors that mediate internal ribosomal entry (3, 4). We report here that we have

[1] The abbreviations used are: eIF, eukaryotic initiation factor; EMCV, encephalomyocarditis virus; PTB, pyrimidine tract binding protein; IRES, internal ribosomal entry site; RBD, RNA binding domain; DMS, dimethylsulfate; CMCT, 1-cyclohexyl-3-(2-morpholino-ethyl)-carbodiimide metho-*p*-toluenesulfonate; nt, nucleotide.

used a combination of chemical and enzymatic protection ("footprinting") assays to map the site in the EMCV IRES that is recognized and bound by eIF4F. This structural element is conserved in the IRESs of several other viruses, including all members of the cardiovirus, aphthovirus, and hepatovirus genera of the Picornaviridae family. The effects of mutations in this structural element on translational activity of these IRESs are consistent with its interaction with eIF4G being a critical step in initiation.

MATERIALS AND METHODS

Plasmids—Plasmids have been described (9, 17, 20, 21). pTE17 contains EMCV nt 378–1155 downstream of a T7 promoter. pTE8 and pTE10 are identical to pTE17 except for deletions of EMCV nt 485–647 and nt 701–763, respectively. pET28(His$_6$-eIF4G$^{457-1396}$) (9) was renamed pET28(His$_6$-eIF4G$^{457-1404}$), reflecting corrections to the sequence of eIF4G (7).

In Vitro Transcription—Plasmids pTE8, pTE10, and pTE17 were linearized by digestion with *Pst*I. Transcription with T7 RNA polymerase and subsequent purification of RNA were done as described previously (17).

Purification of Factors—Native eIF4F and recombinant eIF4A, eIF4B, and eIF4G$^{457-1404}$ and recombinant eIF4A were purified as described elsewhere (9, 17). The *trans*-dominant eIF4A R362Q mutant (22) was a kind gift of N. Sonenberg (McGill University, Montreal).

Assembly of RNA-Protein Complexes—RNP complexes were formed by incubating initiation factors and EMCV IRES transcripts for 5 min at 30 °C in buffer (100 mM potassium acetate, 2 mM magnesium acetate, 2 mM Tris-HCl, pH 7.5, 1 mM dithiothreitol). Reactions contained 1 μg of EMCV RNA (4 pmol) and 1 μg of eIF4G$^{457-1404}$ (10 pmol), 3 μg of eIF4F (13 pmol), 1 μg of eIF4A (22 pmol), 1.5 μg (21 pmol) of eIF4B, and ATP (1 mM), as indicated in the text, in a volume of 20 μl.

Chemical and Enzymatic Footprinting—RNP complexes were probed with RNase V1, DMS, and CMCT as described previously (23). Cleaved or modified sites were identified by primer extension, done using avian myeloblastosis virus reverse transcriptase and the primers 5′-CTCAA-AAGTGAGAGAGTGCGC-3′ (complementary to nt 884–864), 5′-CGC-TTGAGGAGAGCCAT-3′ (complementary to nt 669–653), and 5′-GGG-GTTCCGCTGCC-3′ (complementary to nt 539–526), as appropriate.

Toeprint Analysis of RNP Complexes—Toeprint analysis of EMCV mRNA·eIF4G$^{457-1404}$ complexes was done as described previously (9, 17) using the primer 5′-GTCAATAACTCCTCTGG-3′ (complementary to EMCV nt 957–974).

UV Cross-linking—UV cross-linking of RNP complexes consisting of the EMCV IRES and recombinant eIFs 4A, 4B, and 4G$^{457-1404}$ was done as described previously (9), except that were indicated, DMS was included in reactions at the same concentration as used in probing experiments (23).

RESULTS

eIF4G Binds to the Oligo(A) Loop between the J and K Domains of the EMCV IRES—The structure of the EMCV IRES is shown schematically in Fig. 1. As we have previously shown, eIF4F bound to this IRES arrests primer extension at C^{786} (9, 17). Although we could not exclude that the target site for eIF4F is a complex structure formed by more than one of the principal domains of the IRES, the simplest and most likely possibility was that eIF4G binds to the J-K domain. The results of chemical and enzymatic footprinting presented here are wholly consistent with this hypothesis.

Binary complexes of native rabbit eIF4F or of the recombinant C-terminal eIF4G$^{457-1404}$ fragment of eIF4G and the EMCV IRES were probed with DMS, a reagent specific for unpaired A and to a lesser extent C residues. In both instances the strongest protection sites were in the AAAAA$^{770-774}$ loop at the junction of the J and K domains. In addition, residues A^{687}, A^{688}, and A^{724} were protected from DMS modification by eIF4F and eIF4G$^{457-1404}$ (Figs. 2, *A* and *B*, and 6). Neither eIF4F nor eIF4G$^{457-1404}$ protected residues elsewhere in the IRES (data not shown). DMS is small and can penetrate throughout RNP complexes, so these data strongly suggest that the purine bases of these A residues are bound directly by eIF4G. The protection
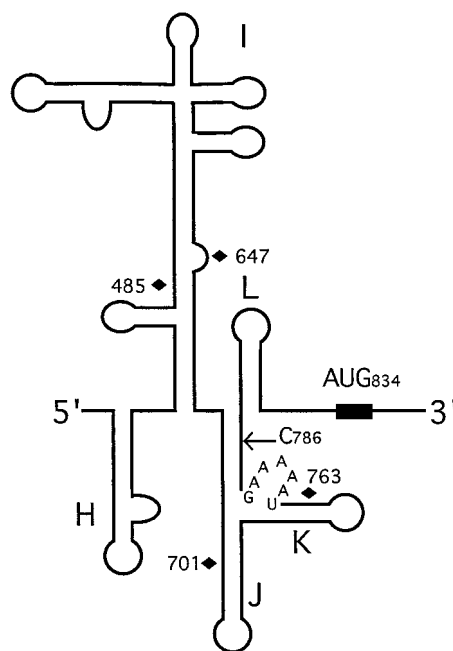

FIG. 1. **Schematic representation of the secondary structure of EMCV IRES.** Domains H to L are named alphabetically. The start codon of the viral polyprotein (AUG$^{834-836}$) is indicated by a *black rectangle*. The position of the stop site (C^{786}) detected previously by primer extension inhibition in the presence of eIF4G (17, 18) is indicated by a *thin arrow*. *Black diamonds* indicate the boundaries of deletions Δ485–647 and Δ701–763 in domains I and J-K, respectively, that were used in this study.

patterns for eIF4F and the RBD-containing fragment of its 4G subunit were identical in this and all other experiments (see below). Therefore, hereafter only data for eIF4G$^{457-1404}$ will be shown.

Binary (IRES·eIF4G$^{457-1404}$) complexes were probed with CMCT, which modifies unpaired U and G residues. A single nucleotide (U^{725}) was protected by eIF4G$^{457-1404}$ from CMCT modification (data not shown). Together, footprinting with DMS and CMCT yielded a comprehensive map of the interaction of eIF4G with unpaired regions of the IRES.

Next, we probed these binary complexes with RNase V1, which cleaves double-stranded and other base paired or stacked RNA. This analysis revealed protection of internucleotide bonds in the J2 and K1 helices (Figs. 2*B*, *lanes 4* and *5*, and 6, *lanes 2* and *3*). These stems flank the oligo(A) loop and with helix J3 form the characteristic bifurcated structure of the J-K domain. In addition, eIF4G$^{457-1404}$ strongly enhanced cleavage of the IRES at G^{766}, C^{784}, and C^{785}. Binding of eIF4G therefore causes conformational rearrangements in the EMCV IRES. The results of footprinting the IRES·eIF4G$^{457-1404}$ complex are summarized in Fig. 7.

Specificity of Interaction of eIF4G with the Oligo(A) Loop Is Determined by Its Structural Context—Specificity of interaction of eIF4G with the EMCV IRES can be inferred from our recent reports (9, 17), in which we found that binding of eIF4G$^{457-1404}$ to the EMCV Δ701–763 deletion mutant and to an AAAAAU^{775} → UA deletion-insertion mutant did not arrest primer extension at C^{786}. These results are consistent with a loss of affinity of eIF4G for the mutant IRESs. The minimal activity of these two mutants in translation initiation strongly supports the functional importance of the interaction of eIF4G with the IRES. To investigate this issue further, footprinting was done on the Δ701–763 mutant in the presence and absence of eIF4G$^{457-1404}$. The oligo(A) loop between J and K domains that is bound by eIF4G in the wild type IRES is intact in this
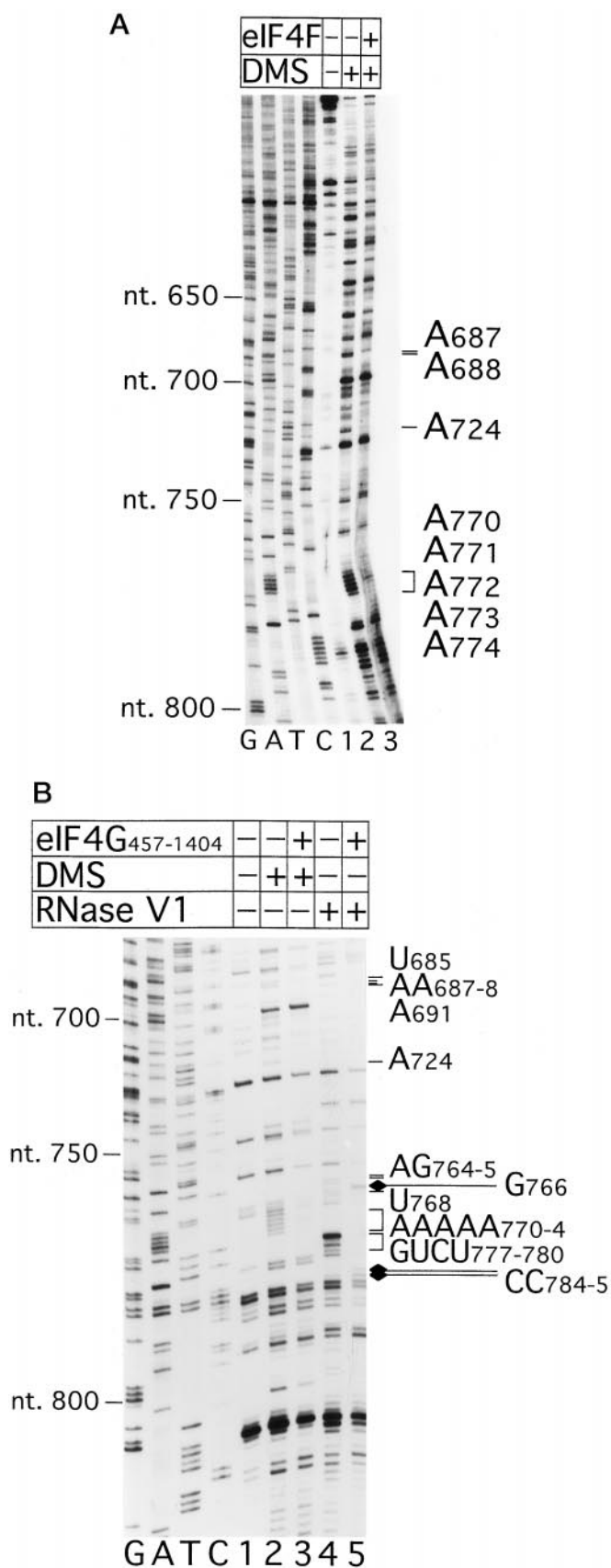
FIG. 2. *A*, chemical footprinting of EMCV domain J-K in complexes formed between eIF4F and EMCV nt 378–1155 RNA. Polyacrylamide-urea gel fractionation of cDNA products obtained after primer extension showing the DMS reactivity of the EMCV IRES either alone (*lane 2*) or complexed with eIF4F (*lane 3*). cDNA products obtained after primer extension of untreated EMCV RNA are shown in *lane 1*. *B*, chemical and enzymatic footprinting of EMCV J-K domain in complexes

mutant (Fig. 3*A*). The A residues in this loop are totally accessible to DMS attack and are therefore still exposed and unpaired (Fig. 3*B*). Nevertheless, they were not protected at all by eIF4G[457–1404] from DMS modification (Fig. 3*B*).

Structural Elements Upstream of the J-K Domain Do Not Affect Binding of eIF4G to the EMCV IRES—As noted above, eIF4G made no specific contact with any part of the IRES other than the J-K domain. Specifically, no protection from chemical or enzymatic modification was detected in the H, I, or L domains (data not shown). The H domain and adjacent upstream residues are bound by PTB, an auxiliary factor in EMCV IRES function (23, 24). However, we could not rule out the possibility that these domains indirectly affect the interaction of eIF4G with the J-K domain. Significantly, no functional role has been ascribed to the large central domain I in various picornaviruses, although mutational analysis has shown that it is important for IRES activity (19, 21, 25–29). We used toeprinting to investigate whether deletion of the upper conserved part of domain I in the EMCV Δ485–647 IRES mutant affected binding of eIF4G[457–1404]. This deletion did not change either the position or intensity of the toeprint at C[786] with respect to the full-length cDNA (Fig. 4). This result indicates that the upper conserved part of domain I does not contribute to the affinity of the eIF4G-EMCV IRES interaction.

The Presence of eIFs 4A and 4B Does Not Change the Pattern of Protection of the EMCV IRES by eIF4G[457–1404]—EMCV IRES-mediated translation initiation requires ATP, eIF4A, and eIF4G, and is augmented by eIF4B (9, 16, 17). In UV cross-linking experiments done using radiolabeled EMCV IRES transcripts, eIF4G[457–1404] strongly enhanced radiolabeling of eIF4A and eIF4B, but eIF4G[457–1404] itself did not become strongly labeled (Fig. 5, *lanes 1–6*). These results are wholly consistent with our previous data (9) and suggest that these three factors form a complex on the EMCV IRES. UV cross-linking of different combinations of these factors to this IRES was not altered in the presence of DMS (Fig. 5, *lanes 1–6* and *7–12*). We therefore used DMS and RNase V1 in footprinting experiments to determine whether eIFs 4A, 4B, and 4G[457–1404] bound to a specific site on the IRES or altered its conformation in any way.

We did not detect any consistent difference in the patterns of chemical and enzymatic modification of the IRES in the presence of eIF4G[457–1404] alone and in combination with eIFs 4A and 4B (*e.g.* Fig. 6). We noted above that the protection patterns due to binding of eIF4G[457–1404] and eIF4F were similar (compare Fig. 2, *A* and *B*). The modification pattern downstream of the eIF4G binding site was similar to that of free RNA (23), irrespective of whether any combination of eIF4A, eIF4B, eIF4G[457–1404], and ATP was present in reactions. This result indicates that domain L, the only stem-loop structure between domain J-K and the initiation codon was not unwound by these factors. This conclusion is consistent with reports that ribosomal initiation complexes bind directly to the initiation codon without scanning from an upstream position (30). The eIF4A subunit of eIF4F normally cycles through the eIF4F

formed between eIF4G[457–1404] and EMCV nt 378–1155 RNA. Polyacrylamide-urea gel fractionation of cDNA products obtained after primer extension showing the sensitivity of the EMCV IRES to modification by DMS (*lanes 2* and *3*) or to cleavage by RNase V1 (*lanes 4* and *5*) either alone (*lanes 2* and *4*) or complexed with eIF4G[457–1404] (*lanes 3* and *5*). cDNA products derived from untreated EMCV RNA are shown in *lane 1* of each panel. A dideoxynucleotide sequence generated with the same primer was run in parallel on each gel. The positions of protected residues are indicated to the *right* of each panel. Sites of enhanced cleavage by RNase V1 are indicated by *black diamonds*. The position of EMCV nucleotides at 50-nt intervals is indicated to the *left* of each panel.

FIG. 3. *A*, secondary structure of the residual J-K domain in the EMCV Δ701–763 deletion mutant, as suggested by probing experiments (21). The oligo(A) loop is shown in *bold*. *B*, chemical footprinting of EMCV J-K domain in complexes formed between eIF4G$^{457-1404}$ and EMCV nt 378–1155 (Δ701–763) mutant RNA. Polyacrylamide-urea gel fractionation of cDNA products obtained by primer extension showing the DMS reactivity of the EMCV IRES either alone (*lane 3*), or complexed with 1 µg (*lane 1*) or 2 µg (*lane 2*) eIF4G$^{457-1404}$. cDNAs derived from untreated EMCV RNA are shown in *lane 4*. A dideoxynucleotide sequence generated with the same primer was run in parallel. The positions of residues that are protected by eIF4G$^{457-1404}$ in the wild type EMCV IRES but not in this mutant are indicated to the *right* of each panel. The position of EMCV nucleotides are indicated to the *left* of each panel.

complex, but once bound, an R362Q eIF4A mutant cannot dissociate from eIF4F and thus acts as a *trans*-dominant inhibitor of its function (16, 31). Substitution of wild type eIF4A by this mutant also had no effect on the pattern of protection caused by eIF4G alone (Fig. 6, *lane 7*).

FIG. 4. **Primer extension analysis done on EMCV nt 378–1155 RNA (lanes *1* and *2*) or on the Δ485–647 domain I deletion mutant (lanes *3* and *4*) in the presence (*lanes 2* and *4*) and absence (*lanes 1* and *3*) of eIF4G$^{457-1404}$, done using a primer annealed to EMCV nt 957–974.** The cDNA product marked C_{786} terminated at this nucleotide.

Taken together, these results indicate that the central RBD-containing domain of eIF4G binds specifically to the EMCV IRES and that the subsequent eIF4G-enhanced binding of eIFs 4A and 4B to the IRES does not result in additional protection of the IRES.

DISCUSSION

We recently found that eIF4G directly recognizes the EMCV IRES and that this interaction is important in recruiting the IRES to ribosomes (9, 17). The results of the footprinting experiments reported here show that the eIF4G binding site consists of an oligo(A) loop and three adjacent helices at the junction of the J and K domain of this IRES (Fig. 7). The bases of the oligo(A) loop are bound directly by eIF4G.

A similar structural element comprising an oligo(A) loop at the junction of three helices occurs at an identical position in the IRESes of many other picornaviruses. They include all cardioviruses, all aphthoviruses, echovirus 22, equine rhinoviruses 1 and 2, and hepatitis A virus (3, 4, 18, 19, 35, 36). The conservation of A residues in the loop of this motif is especially remarkable. Indeed, a single nucleotide substitution (A772C) in the loop strongly impairs EMCV IRES activity (37). The majority of phenotypic reversions of this mutation occurred by restoration of a purine (preferably A) residue in the mutated position (38). In addition to the loop, mutations in adjacent helices (such as deletion of nt 727–730 in the J2 helix) (37) also significantly impair IRES activity. A more extensive deletion (Δ701–760) in this domain totally inactived the IRES (21). The oligo(A) loop in this mutant is still in a single-stranded conformation and is completely accessible to DMS modification (21) but its structural context is quite different from wild type (Fig. 3A). We found that this mutant IRES is unable to bind eIF4G,

FIG. 5. **UV cross-linking of initiation factors to the EMCV IRES.** Recombinant eIF4A (*lanes 1, 3–6, and 8–10*), eIF4B (*lanes 4, 5, 9, and 10*) and eIF4G$^{457-1396}$ (*lanes 2, 3, 5, 7, 8, and 10*) were UV cross-linked to [^{32}P]UTP-labeled EMCV (nt 315–1155) RNA in the presence (*lanes 6–10*) or absence (*lanes 1–5*) of DMS. Samples were digested with cobra venom nuclease and RNases A and T$_1$. The positions of these proteins after separation on a 15% polyacrylamide-SDS gel are shown.
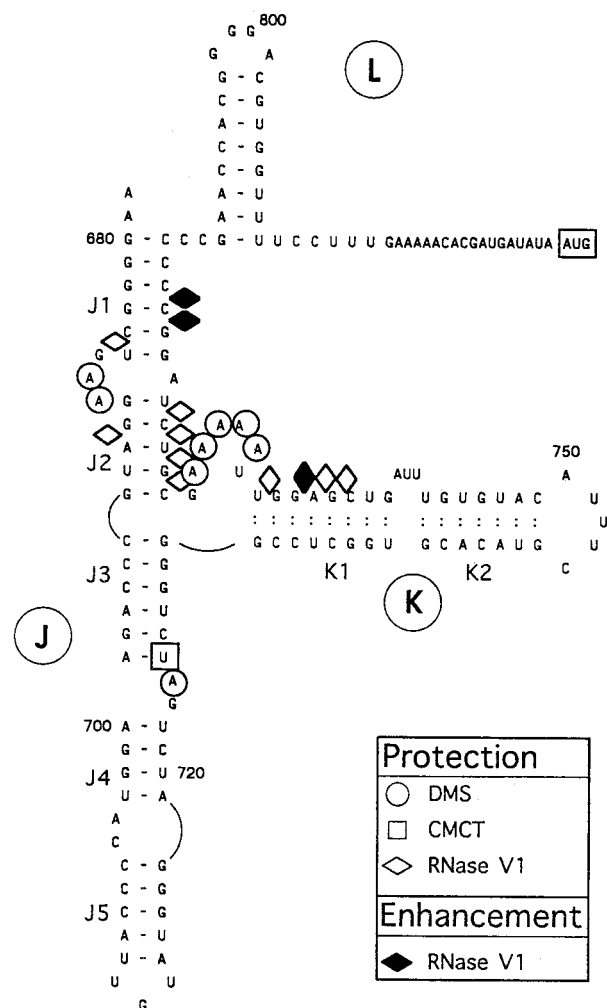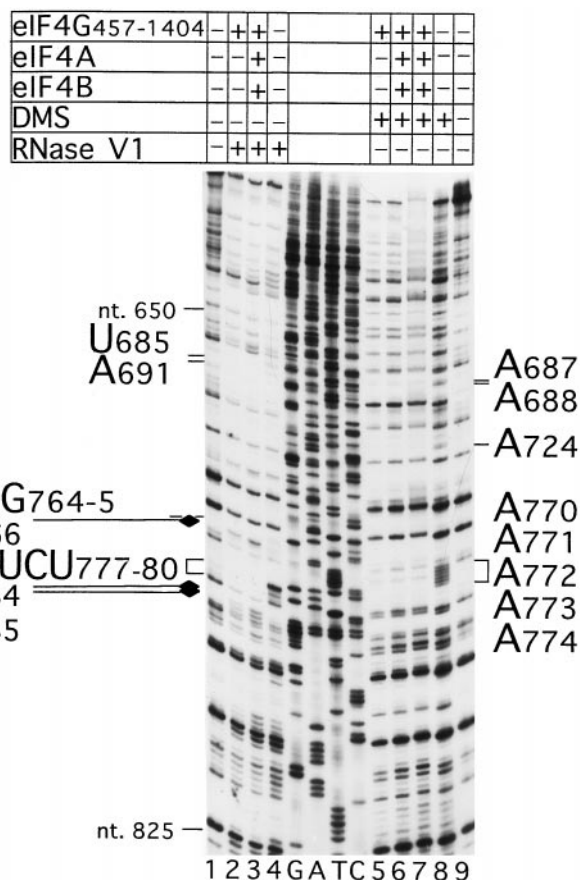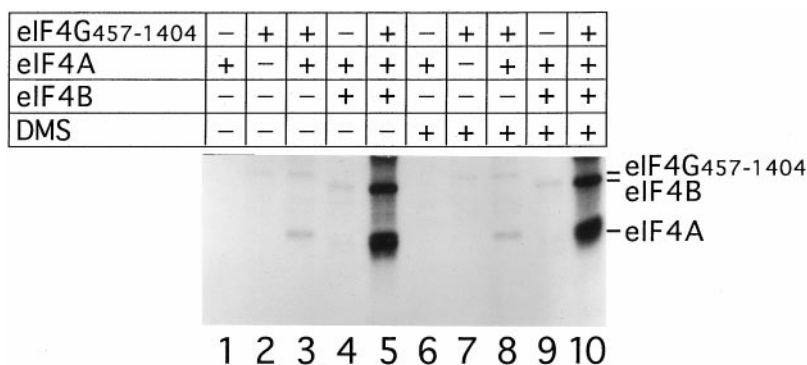

FIG. 6. **Chemical and enzymatic footprinting of the J, K, and L domains of the EMCV IRES in complexes formed between eIF4A, eIF4B, and eIF4G$^{457-1404}$ and EMCV nt 378–1155 RNA.** Polyacrylamide-urea gel fractionation of cDNA products obtained after primer extension showing the sensitivity of the EMCV IRES to cleavage by RNase V1 (*lanes 2–4*) or to modification by DMS (*lanes 5–8*) either alone (*lanes 4 and 8*), complexed with eIF4G$^{457-1404}$ alone (*lanes 2 and 5*), with eIF4G$^{457-1404}$, wild type eIF4A, and eIF4B (*lanes 3 and 6*) or with eIF4G$^{457-1404}$, R362Q mutant eIF4A, and eIF4B (*lane 7*). cDNA products derived from untreated EMCV RNA are shown in *lanes 1 and 9*. A dideoxynucleotide sequence generated with the same primer was run in parallel on each gel. The positions of residues protected from DMS modification are indicated to the *right* of the panel. The position of sites with altered sensitivity to cleavage by RNase V1 are indicated to the *left* of the panel. Sites of enhanced cleavage are indicated by *black diamonds*.

FIG. 7. **Summary of changes in chemical modification by CMCT and DMS and in enzymatic cleavage by RNase V1 of domains J-K-L of the EMCV IRES caused by binding of eIF4G$^{457-1404}$.** These chemical and enzymatic probes are indicated by symbols, as described in the key at *bottom right*. Results are displayed on a secondary structure model (18, 23, 38). The initiation codon is *boxed*.

a result that emphasizes the importance of the structural context surrounding the oligo(A) loop for recognition by eIF4G. The conformation of the eIF4G binding site may be affected by other RNA-binding factors. We have previously suggested that the active conformation of the EMCV IRES which enables it to bind to essential factors such as eIF4G is stabilized by PTB (23). PTB binds to sites at the 5′ and 3′ borders of the EMCV

IRES, including the apical K2 hairpin of the J-K domain. Recent studies that have shown that the dependence of the EMCV IRES on PTB for activity was significantly increased following insertion of a single A residue into the oligo(A) loop (AAAAA$^{770-774}$) (39) are consistent with this proposal.

The organization of the eIF4G binding site on the EMCV IRES is consistent with the general paradigm for the interaction of RBDs with RNA. Their binding normally involves sequence nonspecific electrostatic interactions with the sugar-phosphate backbone of base-paired or stacked RNA, followed

by base-specific interaction with apical or internal RNA loops (32, 33). Bound RNA remains exposed on the β-sheet RNA-binding surface of the RBD and is potentially accessible for interaction with other RNA-binding proteins (12, 33). Our results suggest that eIFs 4A and 4B may bind to the binary (eIF4G·IRES) complex in this way. UV cross-linking of eIF4A and eIF4B to the EMCV IRES is enhanced most significantly by eIF4G when all three factors are present together (9) (Fig. 6). UV cross-linking of eIF4B to the related foot-and-mouth disease virus IRES also requires cytosolic co-factor(s), which we suggest are eIFs 4A and 4G, and involves only the J-K domain (40). Moreover, eIF4A and the EMCV IRES both bind to the same central domain of eIF4G (7, 9). However, the observation that eIFs 4A and 4B did not result in additional protection of binary (eIF4G·IRES) complexes from chemical or enzymatic modification suggests that their interaction with the IRES is transient. During initiation, it may be stabilized by other components of the translation apparatus such as constituents of the 43 S complex.

In this study we found that addition of eIF4A, eIF4B, or both to the binary (eIF4G·IRES) complex did not alter the susceptibility of any part of the IRES to chemical/enzymatic modification, including the hairpin that constitutes domain L between the eIF4G binding site and the initiation codon. This has important implications for the role of eIF4A in recruitment and attachment of a 43 S complex to the EMCV IRES, which therefore does not involve unwinding of mRNA in a classical helicase reaction, but may instead involve rearrangement and accommodation of the IRES in the mRNA-binding cleft of the 40 S subunit. This process of accommodation may require the concerted action of all components needed to form the 48 S preinitiation complex. This model for the activity of the eIF4A subunit of eIF4F may also apply to attachment of 43 S complexes to mRNA in the cap-dependent mode of translation initiation.

Taken together, our results show that eIF4G is an essential factor in EMCV IRES-mediated initiation (17) and suggest that it plays a dual role in this process. One role is selection of EMCV mRNA by specific interaction with the IRES, in a manner analogous to the selection of capped mRNAs by the cap-binding protein eIF4E (9, 17). This results in recruitment of mRNAs to ribosomes by virtue of this interaction and the interaction of eIF4G with eIF3 (6). A second role for eIF4G in IRES-mediated initiation is to recruit eIFs 4A and 4B to the IRES, possibly as a prelude to accommodation of the initiation codon and flanking regions in the mRNA-binding cleft of the 43 S complex.

REFERENCES

1. Merrick, W. C. (1992) *Microbiol. Rev.* **56,** 291–315
2. Rhoads, R. E. (1992) *J. Biol. Chem.* **268,** 3017–3020
3. Jackson, R. J., and Kaminski, A. (1995) *RNA* **1,** 985–1000
4. Hellen, C. U. T., and Wimmer, E. (1995) *Curr. Top. Microbiol. Immunol.* **203,** 31–63
5. Mader, S., Lee, H., Pause, A., and Sonenberg, N. (1995) *Mol. Cell. Biol.* **15,** 4990–4997
6. Lamphear, B. J., Kirchenweger, R., Skern, T. and Rhoads, R. E. (1995) *J. Biol Chem.* **270,** 21975–21983
7. Imataka, H., and Sonenberg, N. (1997) *Mol. Cell. Biol.* **17,** 6940–6947
8. Haghighat, A., and Sonenberg, N. (1997) *J. Biol. Chem.* **272,** 21677–21680
9. Pestova, T. V., Shatsky, I. N., and Hellen, C. U. T. (1996) *Mol. Cell. Biol.* **16,** 6870–6878
10. Yan, R., Rychlik, D., Etchison, D., and Rhoads, R. E. (1992) *J. Biol. Chem.* **267,** 23226–23231
11. Goyer, C., Altmann, M., Lee, H. S., Blanc, A., Deshmukh, M., Woolford, J. L., Trachsel, H., and Sonenberg, N. (1993) *Mol. Cell. Biol.* **13,** 4860–4874
12. Burd, C. G., and Dreyfuss, G. (1994) *Science* **265,** 615–621
13. Rozen, F., Edery, I., Meerovitch, K., Dever, T. E., Merrick, W. C., and Sonenberg, N. (1990) *Mol. Cell. Biol.* **10,** 1134–1144
14. Scheper, G. C., Voorma, H. O., and Thomas, A. A. M. (1992) *J. Biol. Chem.* **267,** 7269–7274
15. Ohlmann, T., Rau, M., Pain, V. M. and Morley, S. J. (1996) *EMBO J.* **15,** 1371–1382
16. Pause, A., Methot, N., Svitkin, Y., Merrick, W. C., and Sonenberg, N. (1994) *EMBO J.* **13,** 1205–1215
17. Pestova, T. V., Hellen, C. U. T., and Shatsky, I. N. (1996) *Mol. Cell. Biol.* **16,** 6859–6869
18. Pilipenko, E. V., Blinov, V. M., Chernov, B. K., Dmitrieva, T. M., and Agol, V. M. (1989) *Nucleic Acids Res.* **17,** 5701–5711
19. Brown, E. A., Day, S. P., Jansen, R. W., and Lemon, S. M. (1991) *J. Virol.* **65,** 5828–5838
20. Borovjagin, A. V., Ezrokhi, M. V., Rostapshov, V. M., Ugarova, T. Y., Bystrova, T. F., and Shatsky, I. N. (1991) *Nucleic Acids Res.* **19,** 4999–5005
21. Evstafieva, A. G., Ugarova, T. Y., Chernov, B. K., and Shatsky, I. N. (1991) *Nucleic Acids Res.* **19,** 665–671
22. Pause, A., and Sonenberg, N. (1992) *EMBO J.* **11,** 2643–2654
23. Kolupaeva, V. G., Hellen, C. U. T., and Shatsky, I. N. (1996) *RNA* **2,** 1199–1212
24. Borovjagin, A. V., Pestova, T. V., and Shatsky, I. N. (1994) *FEBS Lett.* **351,** 299–302
25. Kuhn, R., Luz, N., and Beck, E. (1990) *J. Virol.* **64,** 4625–4631
26. Van der Velden, A., Kaminski, A., Jackson, R. J., and Belsham, G. J. (1995) *Virology* **214,** 82–90
27. Witherell, G. W., Schultz-Witherell, C. S., and Wimmer, E. (1995) *Virology* **214,** 660–663
28. Martínez-Salas, E., Regalado, M. P., and Domingo, E. (1996) *J. Virol.* **70,** 992–998
29. López de Quinto, S., and Martínez-Salas, E. (1997) *J. Virol.* **71,** 4171–4175
30. Kaminski, A., Howell, M. T., and Jackson, R. J. (1990) *EMBO J.* **9,** 3753–3759
31. Yoder-Hill, J., Pause, A., Sonenberg, N., and Merrick, W. C. (1993) *J. Biol. Chem.* **268,** 5566–5573
32. Oubridge, C., Ito, N., Evans, P. R., Teo, C. H., and Nagai, K. (1994) *Nature* **372,** 432–438
33. Allain, F. H. T., Gubser, C. C., Howe, P. W. A., Nagai, K., Neuhaus, D., and Varani, G (1996) *Nature* **380,** 646–650
34. Görlach, M., Wittekind, M., Beckman, R. A., Mueller, L., and Dreyfuss, G. (1992) *EMBO J.* **11,** 3289–3295
35. Hyppia, T., Horsnell, C., Maaronen, M., Khan, M., Kalkinnen, N., Auvinen, P., Linnunen, L., and Stanway, G. (1992) *Proc. Natl. Acad. Sci. U. S. A.* **89,** 8847–8851
36. Wutz, G., Auer, H., Nowotny, N., Grosse, B., Skern, T., and Kuechler, E. (1996) *J. Gen. Virol.* **77,** 1719–1730
37. Hoffman, M. A., and Palmenberg, A. C. (1995) *J. Virol.* **69,** 4399–4406
38. Hoffman, M. A., and Palmenberg, A. C. (1996) *J. Virol.* **70,** 6425–6430
39. Kaminski, A., and Jackson, R. J. (1998) *RNA* **4,** 626–638
40. Meyer, K., Petersen, A., Niepmann, M., and Beck, E. (1995) *J. Virol.* **69,** 2819–2824